RSS-Based Localization using A Single Robot in Complex Environments

Hongzhi Guo, Irvin Quartey, and Cameron Green
Engineering Department
Norfolk State University, VA, 23504, USA
Emails: hguo@nsu.edu, i.quartey@spartans.nsu.edu, c.n.green100164@spartans.nsu.edu

***Abstract*—This paper considers the problem of localizing a static transmitter using a robot with a single receiving antenna and a single communication channel in unknown complex environments. Existing solutions using Time-of-Arrival (TOA) and Angle-of-Arrival (AOA) rely on complex wireless communication systems with multiple receive antennas or multiple communication channels, which are not available for robots with off-the-shelf low-cost radios. This paper develops a localization framework using Received Signal Strength (RSS) to estimate unknown channel model parameters considering multipath fading and spatial-correlated shadowing effects. The robot moves along a predefined trajectory to collect RSS data. AOA information is also estimated and integrated with the robot SLAM (Simultaneous Localization and Mapping) results to improve the localization accuracy. Numerical simulations and experiments in an indoor environment are conducted. Results show that 90% of the estimation error is smaller than 2 m to localize a randomly placed transmitter in a 10×10 m^2 area.**

***Index Terms*—Complex environment, estimation, localization, received signal strength, robot, sensor data processing, wireless channel model.**

I. Introduction

Low-cost wireless localization using mobile robots plays an important role in target tracking, rescue, robot coordination, and wireless sensing [1], [2]. In this paper, we consider the problem of localizing a wireless transmitter using a single robot in a complex unknown environment with Received Signal Strength (RSS) measurements.

Existing high-precision localization mainly use two approaches [3]–[9]. First, machine learning with location-based features are used. It is applicable for environments with prior knowledge. Also, the wireless environment is stable and the features are not time-varying. Second, various location-related information such as Time-Of-Arrival (TOA) and Angle-Of-Arrival (AOA) are collected by multi-antenna communication systems to estimate the transmitter's location. To obtain TOA and AOA information, it requires complex devices that most tiny low-cost robots do not have.

Without multiple antennas or prior knowledge of the environment, a mobile robot cannot use information of TOA, AOA, and prior location-related features. It faces the following challenges to localize a transmitter. First, the robot has to use RSS measurements that is affected by multipath fading, shadowing effects, distance, RF environment, and transmission power. Despite that RSS data can be collected by most of the wireless radios such as Wi-Fi and LoRa, the localization accuracy is lower compared with TOA, AOA, and feature-based solutions. Moreover, the robot has to move along several waypoints to emulate an antenna array to increase the space diversity. Second, the RSS-based localization relies on accurate channel models, which are not available in unknown complex environments. Without an accurate channel model, the estimation of transmitter location is challenging.

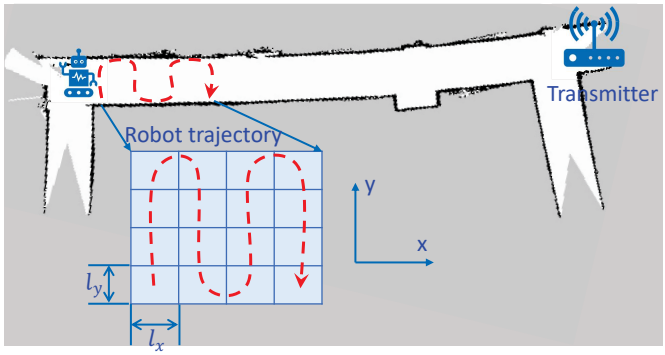

Fig. 1. Robot trajectory (red). The corridor is divided into virtual grids. A robot maps the environment and localize the transmitter simultaneously.

RSS-based localization using anchor sensors with unknown channel parameters has been studied in [10]–[14]. These approaches are based on widely distributed anchor sensors. The received RSS data are used to localize or track targets using various localization algorithms. In this paper, a mobile robot is used to localize a transmitter without any support from anchor sensors.

In this paper, a mobile robot moves along a predefined trajectory with several waypoints to collect RSS data, as shown in Fig. 1. The robot has to move in a relatively small area to collect sufficient data to estimate the channel unknown parameters, such as the correlated shadowing effects and multipath fading. An optimization problem is formulated to estimate the path loss exponent and the distance from transmitter. The semidefinite programming is employed to obtain an approximation of the solution. Mobile robots are usually equipped with various sensors such as LiDAR for

This work was supported in part by the National Science Foundation under grant no. CNS1947748.

SLAM (Simultaneous Localization And Mapping), which can be leveraged to gather more environmental information. Based on the RSS data and channel estimation results, we obtain the AOA estimation, which is used jointly with SLAM results to further improve the localization accuracy. The contributions of this paper include

- First, we develop a framework to estimate channel spatial correlation, path loss exponent, and the distance from transmitter using a mobile robot with a single receive antenna and a single wireless channel.
- Second, we design an algorithm to jointly estimate the angle of arrival and transmitter location, which is subsequently integrated with the robot SLAM to improve the localization accuracy.
- Third, we perform numerical simulations and compare our approach with existing solutions. Moreover, we collect RSS data using a Wi-Fi router and a TurtleBot3 Waffle Pi robot with Wi-Fi modules and verify the proposed solution.

The rest of this paper is organized as follows. In section II, we present the related works. After that, we introduce the RSS-based localization algorithm using a single robot in Section III. The numerical simulations and experiments are given in Section IV. Finally, this paper is concluded in Section V.

In this paper, we use boldface lower-case letters to denote column vectors, boldface upper-case letters to denote matrices. For a vector and a matrix, we use $(\cdot)^t$ to denote transpose. The inverse and trace of a matrix $\boldsymbol{A}$ are denoted by $(\boldsymbol{A})^{-1}$ and $\mathrm{Tr}(\boldsymbol{A})$, respectively. The i^{th} entry of a vector $\boldsymbol{a}$ is $[\boldsymbol{a}]_i$ and the (i,j) entry of a matrix $\boldsymbol{A}$ is $[\boldsymbol{A}]_{i,j}$. For a matrix $\boldsymbol{A}$, the i^{th} column is $[\boldsymbol{A}]_{:,i}$ and the i^{th} row is $[\boldsymbol{A}]_{i,:}$.

II. Related Work

The state-of-the-art localization accuracy in complex indoor environment is at decimeter level [3]–[5]. The technology relies on multiple Wi-Fi access points with multiple antennas and multiple channels to estimate TOA and AOA. However, for a single robot with an antenna and a simple receiver, it cannot obtain this information directly.

Data-driven localization algorithms use pre-collected data with known locations to build a database or train a machine learning model. Real-time data samples are input into machine learning models, which can output predicted locations [5]–[9]. Similar to most of the data-driven approaches, the above algorithms require a significant amount of pre-collected data. Although the accuracy is attractive, they cannot be applied to complex dynamic environments, where the trained model cannot be adaptive to strong environment dynamics. Moreover, it is not always possible to collect data before applying the localization algorithms. Under these conditions, it is not straightforward to employ data-driven approaches.

RSS-based localization algorithms require simple low-cost hardware, which is suitable for most sensors and robots. On the other hand, its localization accuracy is lower compared with the aforementioned TOA, AOA, and data-driven approaches. For example, existing RSS-based algorithms can achieve a localization accuracy of 1 to 5 m in indoor environments [10], [15], which is much higher than the decimeter level accuracy. The RSS-based localization accuracy is highly affected by the accuracy of the channel model. In dynamic complex environments, it is not wise to use a static channel model since it cannot effectively characterize the wireless environment. Therefore, the localization problem is usually jointly solved with the estimation of channel models, e.g., localization with unknown transmit power and/or unknown path loss exponent [10]–[14]. The dynamic environment is taken into account by estimating the unknown channel model parameters. This problem is challenging due to the increase of unknown parameters. Various approaches, including MMSE (minimum mean square error), Least Squares, Maximum Likelihood, and Semidefinite Relaxation, are employed to solve this problem and the accuracy is similar to RSS-based algorithms with known channel parameters. This approach uses multiple anchors with known locations to collect RSS data. The anchors are placed widely separated (mutual distance is longer than/around 10 m) to collect independent information and the target is assumed to be in the area that is covered by anchors. This is different from the use of a single robot where anchors are not available.

More relevantly, localization and target searching using a single robot have been studied in [16]–[19]. A robot is employed to localize RFID tags in [16]–[18]. The localization algorithm is based on the phase information at different locations. By obtaining the spatial-domain cross-correlation, one can estimate the tag's location. The approach relies on signal phases, which is fundamentally different from this paper. In [19], robots are used as transmitters and receivers to localize static objects and track moving targets. RSS data are collected by one or multiple receivers to increase the diversity. AoA is first estimated and then used to estimate the target locations. Various experiments show that the algorithm can accurately localize static objects and track moving targets. A path loss channel model is not used and the localization is performed within an area smaller than 10 m$\times$10 m. Since we only have one receiver and the range can be longer than 10 m, the approach in [19] cannot be directly applied.

III. System Model and Localization Framework Design

We consider the problem that a single robot localizes a static transmitter at location $\boldsymbol{s} \in \mathbb{R}^{2\times 1}$ in a 2D complex environment. The robot moves along a predefined trajectory with N_l waypoints, which are organized as grids, as shown in Fig. 1, to collect multiple measurements in order to emulate an antenna array. Waypoints along the trajectory are $\boldsymbol{L} = [\boldsymbol{r}_1, \boldsymbol{r}_2, \cdots, \boldsymbol{r}_{N_l}]$, where $\boldsymbol{r}_i \in \mathbb{R}^{2\times 1}$. At each location $\boldsymbol{r}_i$, the robot collects N_m RSS measurements, which are $\boldsymbol{P}_r = [\boldsymbol{p}_r(\boldsymbol{r}_1), \boldsymbol{p}_r(\boldsymbol{r}_2), \cdots, \boldsymbol{p}_r(\boldsymbol{r}_{N_l})]$, where $\boldsymbol{p}_r(\boldsymbol{r}_i) \in \mathbb{R}^{N_m\times 1}$.

A. Channel Model

In practice, when a robot is in an unknown or dynamic complex environment, it does not have the knowledge of wireless channel parameters. In particular, the received signal power at $\boldsymbol{r}_i$ can be written as

$$p_r(\boldsymbol{r}_i) = p_r(\boldsymbol{r}_0) - 10\alpha \log_{10} \frac{d_i}{d_0} + u(\boldsymbol{r}_i) + w(\boldsymbol{r}_i), \quad (1)$$

where $p_r(\boldsymbol{r}_0)$ is the received power at a reference location $\boldsymbol{r}_0$, which is usually considered as 1 m away from the transmitter, α is the path loss exponent, $d_i = \|\boldsymbol{r}_i - \boldsymbol{s}\|$, $d_0 = \|\boldsymbol{r}_0 - \boldsymbol{s}\|$, $u(\boldsymbol{r}_i) \in \mathcal{N}(0, \sigma^2)$ is a Gaussian random variable due to multipath fading, and $w(\boldsymbol{r}_i)$ is a random variable due to shadowing effects.

Note that, we consider the multipath fading is spatially independent since it decorrelates fast. The shadowing effect is usually spatially correlated [20], [21], which can be modeled as an exponentially-decaying function:

$$\mathbb{E}(w(\boldsymbol{r}_i), w(\boldsymbol{r}_j)) = \gamma \cdot \exp\left(\frac{-\|\boldsymbol{r}_i - \boldsymbol{r}_j\|}{\eta}\right), \quad (2)$$

where γ is the shadowing power and η is the correlation distance. We assume $[w(\boldsymbol{r}_1), w(\boldsymbol{r}_2), \cdots, w(\boldsymbol{r}_{N_m})]^t$ are zero-mean Gaussian random variables with covariance $\boldsymbol{R}$, where $[\boldsymbol{R}]_{i,j} = \mathbb{E}(w(\boldsymbol{r}_i), w(\boldsymbol{r}_j))$ which is given in Equ. (2).

Localization considering spatial correlation is studied in [22], but the channel is known. In this paper, we consider the knowledge of channel parameters is not available, i.e., α, σ, γ, and η are unknown. However, we assume the transmission power is known ($p(\boldsymbol{r}_0)$ and d_0). In practice, when we localize a device with standard communication protocols, usually, we can find the transmission power. This information can also be sent via wireless communication.

Direct positioning by jointly estimating all the unknown parameters in conjunction with the transmitter location $\boldsymbol{s}$ is challenging due to the nonlinear logarithm and exponential functions. Although various approximations can linearize the exponential functions, they are based on assumptions of roughly knowing those parameters or having prior knowledge. In this paper, we only have RSS samples without any other prior information. The estimation is divided into three steps, namely, covariance and multipath fading estimation, path loss exponent estimation, and AOA and location estimation.

B. Shadowing and Multipath Fading

First, we estimate σ, γ, and η. These parameters are affected by the environment which can vary significantly at different locations. Considering them as global parameters may result in a low accuracy. In this paper, the robot moves in a relatively small area to collect RSS data following a predefined trajectory, as shown in Fig. 1. The robot moves to cover the virtual grids with length l_x and width l_y. Note that, l_x can be different from l_y depending on the space and the distance from transmitter. In each grid, the robot collects N_m measurements of RSS. The number of columns N_c and the number of rows N_r are variables which are determined by the environment, e.g., walls may prevent the robot from moving in the x or y direction. Without the knowledge of distance or path loss exponent, we cannot use typical estimation algorithms such as least squares to obtain σ and γ. To address this problem, the robot uses local RSS measurements within a small area, and periodically updates its estimation using the following approach.

First, the measurements are centered using

$$\hat{\boldsymbol{p}}_r(\boldsymbol{r}_i) = \boldsymbol{p}_r(\boldsymbol{r}_i) - \tilde{p}, \text{ for } i = 1, 2, \cdots, N_l \quad (3)$$

where $\tilde{p} = \mathbf{1}^t(\sum_{i=1}^{N_l} \boldsymbol{p}_r(\boldsymbol{r}_i))/N_l N_m$ and $\mathbf{1}$ is a column vector with all 1 elements. Since the measurements are collected within a small area, all the grids have similar distance to transmitter. By removing $\tilde{p}$, only the multipath fading and shadowing effect are kept. Then, we can obtain $\sigma^2 + \gamma \approx \text{Tr}(\boldsymbol{K}_R)/N_t$ where $\boldsymbol{K}_R = \mathbb{E}(\hat{\boldsymbol{R}}\hat{\boldsymbol{R}}^t)$ and $\hat{\boldsymbol{R}} = [\hat{\boldsymbol{p}}_r(\boldsymbol{r}_1), \hat{\boldsymbol{p}}_r(\boldsymbol{r}_2), \cdots, \hat{\boldsymbol{p}}_r(\boldsymbol{r}_{N_l})]$. By using the above equation, we can only find the summation of σ^2 and γ. To find their individual values and η, we need to use the off-diagonal elements in the covariance matrix.

We rewrite Equ. (2) in log scale, which is

$$\log\left(\mathbb{E}(w(\boldsymbol{r}_i), w(\boldsymbol{r}_j))\right) = \log\gamma - \frac{\|\boldsymbol{r}_i - \boldsymbol{r}_j\|}{\eta} \quad (4)$$

$$= x_1 - \|\boldsymbol{r}_i - \boldsymbol{r}_j\| x_2, \quad (5)$$

where $x_1 = \log\gamma$ and $x_2 = 1/\eta$. Thus, for the i^{th} row in $\boldsymbol{K}_R$ we have $\boldsymbol{X}_i \boldsymbol{x}_i = \boldsymbol{k}_{Ri}$, where

$$\boldsymbol{X}_i = \begin{bmatrix} 1 & -\|\boldsymbol{r}_i - \boldsymbol{r}_1\| \\ 1 & -\|\boldsymbol{r}_i - \boldsymbol{r}_2\| \\ \vdots & \vdots \\ 1 & -\|\boldsymbol{r}_i - \boldsymbol{r}_{N_l}\| \end{bmatrix}, \quad \boldsymbol{k}_{Ri} = \begin{bmatrix} [\boldsymbol{K}_R]_{i,1} \\ [\boldsymbol{K}_R]_{i,2} \\ \vdots \\ [\boldsymbol{K}_R]_{i,N_l} \end{bmatrix} \quad (6)$$

and $\boldsymbol{x}_i = \begin{bmatrix} x_{1,i} & x_{2,i} \end{bmatrix}^t$. Note that, in $\boldsymbol{X}_i$ and $\boldsymbol{k}_{Ri}$, $\boldsymbol{r}_i \neq \boldsymbol{r}_j$ and the diagonal entry of $\boldsymbol{K}_R$ is not included. Then, we can obtain

$$\boldsymbol{x}_i = (\boldsymbol{X}_i^t \boldsymbol{X}_i)^{-1} \boldsymbol{X}_i^t \boldsymbol{k}_{Ri}. \quad (7)$$

Note that, σ^2 is nonnegative. We also use a ReLU rectifier for $\boldsymbol{K}_R$ to change any negative values to 0. Due to multipath fading and shadowing effects, the estimated $\boldsymbol{x}_i$ may not be meaningful, i.e., $x_{2,i}$ should be real positive and $x_{1,i}$ should be real, otherwise, we cannot obtain a meaningful result. To eliminate meaningless results, we find the summation of estimated $x_{1,i}$ and $x_{2,i}$. Then, we update x_1 and x_2 using the mean value of $x_{1,i}$ and $x_{2,i}$, respectively. Finally, the estimated values are $\gamma = \exp(x_1)$, $\eta = 1/x_2$, and $\sigma^2 = \max(0, \text{Tr}(\boldsymbol{K}_r)/N_t - \exp(x_1))$. Substituting these parameters into Equ. (2), we can obtain the covariance matrix $\boldsymbol{R}$. However, the above estimation is based on local observations. As the robot moves away from the area, the estimation may not be accurate. Therefore, the robot has to update its estimation periodically.

C. Path Loss Exponent and Distance

Jointly estimating the path loss exponent α and the distance between the transmitter and the receiver is a challenging problem. Overestimating of α results in underestimation of the distance, vice versa. Existing solutions use approximations to first narrow the solution search space, then use the initial estimated results to improve the accuracy of the approximation [13]. Also, constraints are added to regulate the solution [10]. In this paper, we do not consider any prior knowledge of the environment and the solution is based on searching for optimal α in $[1, \infty)$.

First, assume that we have an estimation of α, which is $\hat{\alpha}$. Then, using Equ. (1), we can estimate the distance by solving the following problem:

$$\text{P1 } (\hat{\alpha}, \boldsymbol{d}): \min_{\boldsymbol{d},\boldsymbol{s}} \ f(\boldsymbol{d}) = (\boldsymbol{p}_r(\boldsymbol{r}_0) - \boldsymbol{p}_m - 10\hat{\alpha}\log_{10}\boldsymbol{d})^t \times \boldsymbol{R}^{-1}(\boldsymbol{p}_r(\boldsymbol{r}_0) - \boldsymbol{p}_m - 10\hat{\alpha}\log_{10}\boldsymbol{d}) \quad (8)$$

$$s.t. \ \|\boldsymbol{s} - \boldsymbol{r}_i\| = [\boldsymbol{d}]_i, \ \text{for } i = 1, \ 2, \cdots, N_l; \quad (9)$$

where $\boldsymbol{p}_r(\boldsymbol{r}_0) = p_r(\boldsymbol{r}_0)\mathbf{1}$ and $\boldsymbol{p}_m = [\mathbb{E}(\boldsymbol{p}_r(\boldsymbol{r}_1)), \mathbb{E}(\boldsymbol{p}_r(\boldsymbol{r}_2)), \cdots, \mathbb{E}(\boldsymbol{p}_r(\boldsymbol{r}_{N_l}))]^t$. Directly solving the above problem is challenging. Since we mainly estimate the distance based on the path loss exponent, we move $\boldsymbol{d}$ outside of the logarithm and change the problem to the following format:

$$\min_{\boldsymbol{d},\boldsymbol{s}} \ (\boldsymbol{d} - \boldsymbol{y})^t \boldsymbol{R}^{-1}(\boldsymbol{d} - \boldsymbol{y}) \quad (10)$$

$$s.t. \ \|\boldsymbol{s} - \boldsymbol{r}_i\| = [\boldsymbol{d}]_i, \ \text{for } i = 1, \ 2, \cdots, N_t \quad (11)$$

$$\boldsymbol{y} = 10^{\frac{\boldsymbol{p}_r(\boldsymbol{r}_0) - \boldsymbol{p}_m}{10\hat{\alpha}}}, \quad (12)$$

where $\boldsymbol{y}$ can be considered as an estimation of $\boldsymbol{d}$. We implicitly assume $d_0 = 1$ m. We use the Semidefinite Relaxation [23] to obtain an approximation of the solution. The problem is reformulated as

$$\text{P2 } (\hat{\alpha}, \boldsymbol{d}): \min_{\boldsymbol{d},\boldsymbol{s},\boldsymbol{D},y_s} \ \text{Tr}(\boldsymbol{D}\boldsymbol{R}^{-1}) - 2\boldsymbol{y}^t\boldsymbol{R}^{-1}\boldsymbol{d} \quad (13)$$

$$s.t. \ [\boldsymbol{D}]_{i,i} = y_s - 2\boldsymbol{s}^t\boldsymbol{r}_i + \boldsymbol{r}_i^t\boldsymbol{r}_i \quad (14)$$

$$[\boldsymbol{D}]_{i,j} \geq |y_s - \boldsymbol{s}^t(\boldsymbol{r}_i + \boldsymbol{r}_j) + \boldsymbol{r}_i^t\boldsymbol{r}_j|, \ \text{for } i \neq j \quad (15)$$

$$\begin{bmatrix} 1 & \boldsymbol{d}^t \\ \boldsymbol{d} & \boldsymbol{D} \end{bmatrix} \succeq 0 \quad (16)$$

$$\begin{bmatrix} \boldsymbol{I}_2 & \boldsymbol{s} \\ \boldsymbol{s}^t & y_s \end{bmatrix} \succeq 0; \quad (17)$$

where $\boldsymbol{I}_2$ is a 2×2 identity matrix. In the constraints, y_s is a variable used to constrain the norm of transmitter location. Semidefinite Relaxation is an approximation, and the solution may not be exact. Given $\hat{\alpha}$, the solution to the above problem obtains the optimal $\boldsymbol{d}$ and $\boldsymbol{s}$, but it is not clear what the optimal $\hat{\alpha}$ is. To address this problem, we search the optimal α starting from 1.

Due to Equ. (1), the optimal combination of $\hat{\alpha}$ and $\boldsymbol{d}$ should minimize $f(\boldsymbol{d})$. We use a gradient decent algorithm to find $\hat{\alpha}$ and the associated distance $\boldsymbol{d}$. We increase $\hat{\alpha}$ by a step Δ if the newly obtained $f(\boldsymbol{d})$ is smaller than the previous value. This ensures that $f(\boldsymbol{d})$ keeps decreasing until the minimum value is obtained. The accuracy can be adjusted by changing Δ. A summary of the algorithm to obtain the estimated α, $\boldsymbol{d}$, and $\boldsymbol{s}$ is given in Algorithm 1. Although P2$(\hat{\alpha}, \boldsymbol{d})$ can directly generate an estimation of the transmitter location $\boldsymbol{s}$, its accuracy can be further improved by the use of other sensing information such as SLAM.

Algorithm 1: Optimal α

Input: $\boldsymbol{P}_r$, $p_r(\boldsymbol{r}_0)$, d_0
Output: α, $\boldsymbol{d}$, $\boldsymbol{s}$

Initialization: $\alpha_1 = \alpha_2 = 1$; Δ = 0.1;
Solve P2 $(\alpha_1, \boldsymbol{d}_1)$;
$f_1 = f(\boldsymbol{d}_1)$ // Equ. (8)
$f_2 = f_1$; $\boldsymbol{d}_2 = \boldsymbol{d}_1$; $\boldsymbol{s}_2 = \boldsymbol{s}_1$;
while $f_1 \geq f_2$ **do**
    $f_1 = f_2$;
    $\boldsymbol{d}_1 = \boldsymbol{d}_2$; $\boldsymbol{s}_1 = \boldsymbol{s}_2$;
    $\alpha_1 = \alpha_2$;
    $\alpha_2 = \alpha_1 + \Delta$;
    Solve P2 $(\alpha_2, \boldsymbol{d}_2)$;
    $f_2 = f(\boldsymbol{d}_2)$;
end while
$\alpha = \alpha_1$; $\boldsymbol{d} = \boldsymbol{d}_1$; $\boldsymbol{s} = \boldsymbol{s}_1$.

D. AOA and Location

Most of the robots use SLAM for navigation, and robotic sensors such as LiDAR are ubiquitous. Although wireless channel parameters are unknown, the robot can sense the surrounding environment using SLAM, which can be used together with the estimated channel parameters and distances to obtain the location. Next, we refine the localization results based on SLAM maps generated by robot SLAM applications. If $\hat{\alpha}$ is large, it means the signal experiences significant attenuation which can be caused by the non-line-of-sight (NLOS) propagation. The path loss exponent for NLOS is usually higher than 3 [24], [25]. The LOS and NLOS can be distinguished by using machine learning-based solutions [26]. In this paper, when $\hat{\alpha} > 2.5$, we consider the search is performed on a whole 2D plane and we use $\boldsymbol{s}$ as the estimated location. When $\hat{\alpha} \leq 2.5$, there is a strong signal path, and the transmitter location should be in the open space detected by SLAM.

As shown in Fig. 2, using the SLAM map and the estimated distance, we can obtain an area that the transmitter may locate in, which is denoted as $\mathcal{A}$. As shown in Fig. 2, when the space is constrained and $\hat{\alpha} \leq 2.5$, the search area is within one or multiple sectors with angle θ_s. If $\boldsymbol{s}$ also locates in this area, we can use it as the estimated location. Otherwise, we need search for the most likely location in this area. The distance d is measured from each waypoint and it is extracted from $\boldsymbol{d}$. The estimation divides the sector equally into N_θ segments.

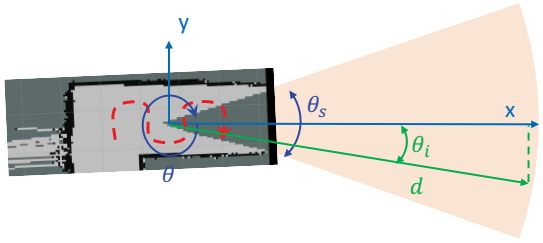

Fig. 2. Illustration of the search area with estimated distance d and SLAM map. The sector with angle θ_s is the search area. Given a specific angle θ_i and distance d, the source location can be estimated. The angle is measured clockwise.

Algorithm 2: Localization Algorithm

Input: $\boldsymbol{P}_r$, $p_r(\boldsymbol{r}_0)$, d_0, $\mathcal{A}$
Output: $\boldsymbol{s}$

Estimate σ, γ, η using Equ. (3) to (7);
Estimate $\hat{\alpha}$, $\boldsymbol{d}$, and $\boldsymbol{s}$ using Algorithm 1;
if $\hat{\alpha} > 2.5$ *or* $\boldsymbol{s} \in \mathcal{A}$ **then**
    Return $\boldsymbol{s}$;
else
    Determine θ_s based on the boundaries;
    Estimate updated $\boldsymbol{s}$ using Equ. (18) to (21);
end if

The reference point for the angle can be chosen as one of the waypoints.

Given an angle θ_i, the estimated location of transmitter is

$$\boldsymbol{s}_{i,j} = \boldsymbol{r}_r + \begin{bmatrix} \cos\theta_i \\ -\sin\theta_i \end{bmatrix} \rho_i, \tag{18}$$

where $\boldsymbol{r}_r$ is the location of the reference waypoint and ρ_i is an unknown variable denoting the distance along the direction of θ_i. Based on the following relation $\|\boldsymbol{s}_{i,j} - \boldsymbol{r}_j\| = [\boldsymbol{d}]_j$, we can obtain ρ_i, which is

$$\rho_i = \frac{1}{2}\left[-C_1 + \sqrt{C_1^2 - 4(\|\boldsymbol{r}_r - \boldsymbol{r}_j\|^2 - [\boldsymbol{d}]_j^2)}\right], \tag{19}$$

where

$$C_1 = 2(\boldsymbol{r}_r - \boldsymbol{r}_j)^t \begin{bmatrix} \cos\theta_i \\ -\sin\theta_i \end{bmatrix}, \tag{20}$$

and $j = 1, 2, \cdots, N_l$.

Since the estimation at each waypoint is equally important, we use the mean value. The estimated transmitter location is $\boldsymbol{s}_i = \sum_{j=1}^{N_l} \boldsymbol{s}_{i,j}/N_l$. By substituting $\boldsymbol{s}_i$ into Equ. (9), we can obtain $\boldsymbol{d}$. Then, using Equ. (8), we can obtain $\{f(\boldsymbol{d})|\theta_i, \boldsymbol{s}_i\}$. The ultimate estimated location is

$$\hat{\boldsymbol{s}} = \arg\min_{\boldsymbol{s}_i} \{f(\boldsymbol{d})|\theta_i, \boldsymbol{s}_i\}. \tag{21}$$

The localization algorithm is summarized in Algorithm 2, including the covariance estimation, path loss exponent and distance estimation, and the AOA and location estimation.

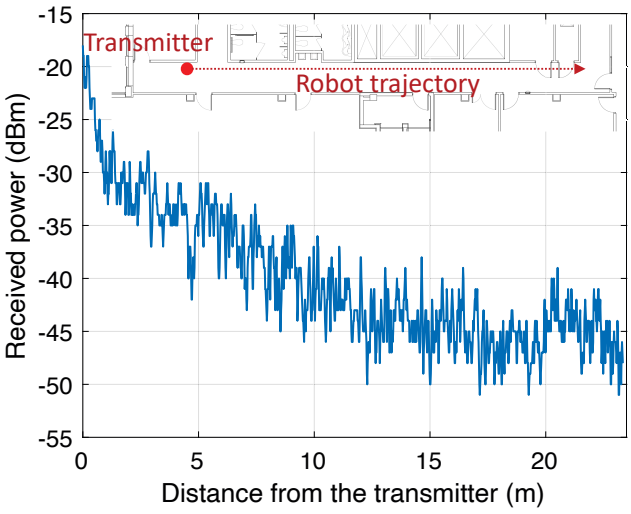

Fig. 3. Received power by a robot in a corridor on the 4th floor of Robinson Technology Center at Norfolk State University. The transmitter is a Wi-Fi router. Received power is measured while the robot is moving.

E. Impact of Distance

The localization accuracy is affected by the robot trajectory in Fig. 1. The design of the trajectory relies on obtaining optimal l_x and l_y. However, the use of l_x and l_y is constrained by the environment. Moreover, the values of l_x and l_y are affected by the distance between the transmitter and the robot. In Fig. 3, we show the measured received power by a mobile robot. The trajectory of the robot is shown in the upper part of the figure.

As we can see, in such an indoor environment, the received power reduces significantly within the first 5 m. As the distance increases, the path loss exponent decreases. Especially between 15 m and 20 m, the received power does not demonstrate an obvious decrease. As shown in the floor plan, this is the intersection area of two corridors. Signals are affected by multipath fading and shadowing significantly. In free space, the path loss exponent is 2, while in the corridor, the path loss exponent is around 1.5 to 2 due to the guided environment [25]. When the distance is longer than 10 m, the change of the mean received power in 1 m becomes small. If the robot moves in such a small area, it cannot collect sufficient spatial information to estimate the distance and path loss exponent.

To obtain sufficient information, the robot has to move in a larger area when the distance from the transmitter is large. On the contrary, the robot can collect sufficient information in a small area when the distance from the transmitter is short. We define a threshold of the received power p_{th}. When the mean received power is larger than p_{th}, the robot will expand its moving area to collect more information, whereas when the mean received power is smaller than p_{th}, the robot moves in a small area to collect information. In our experiment, we notice that -40 dBm is a reasonable p_{th} value for a Wi-Fi router.

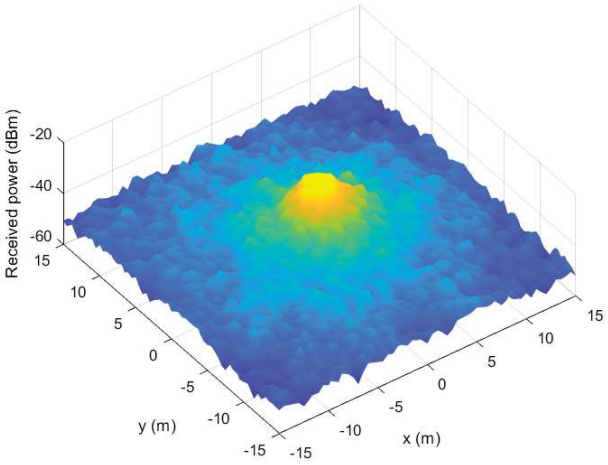

Fig. 4. Simulated received power in a 15×15 m^2 area. The transmitter is at (0,0) with transmission power of -25 dBm. The parameters are γ=2, η=1, σ=1, and α=2.

IV. Numerical Simulation and Experiments

In Fig. 4, we show an example of received power distribution. As we can see, when the robot is close to the transmitter, the received power has a significant decrease and the robot can collect sufficient information to estimate the transmitter's location. As the distance increases beyond 5 m, the change of the received power becomes small within 1 m. Even worse, due to the multipath fading and shadowing effects, the change of the received power becomes random. Note that, in Fig. 4, the received power at (0, 0) is considered as the same as the transmission power.

The localization error is defined as $e = \|\hat{\boldsymbol{s}} - \boldsymbol{s}\|$, which is the distance between estimated location and the real location. First, we consider $l_x = l_y = 0.6$ m and the number of grids in Fig. 1 are 5 and 5 in x and y direction, respectively, i.e., $N_c = N_r = 5$. In the following simulations, $\alpha = 1.5$, $\sigma^2 = 1$, $\gamma = 2$, and $\eta = 1$. Models based on these parameters can better approximate the measured data. Since our experiment is conducted in an indoor environment, the path loss exponent along a corridor is smaller than 2. The center of the robot's trajectory grids is located at the origin, as shown in Fig. 7. At each waypoint, the robot collects 10 measurements. We consider the sources are randomly located in four different squares with edge lengths 5 m, 10 m, 15 m, and 20 m, respectively, as shown in Fig. 7. We run 100 simulations for each scenario and plot the CDF (cumulative distribution function) of the localization error. As shown in Fig. 5, when transmitters are randomly placed in a square with 5 m edge, around 90% of the localization has an error that is smaller than 1 m, while for 10 m, this number is increased to around 5 m. For 15 m and 20 m, about 90% and 70% of the localization errors are smaller than 10 m, respectively. This is consistent with our analysis that the RSS-based localization accuracy reduces as the distance increases.

For the long-distance localization, the robot can move in a larger area to collect more spatial information. In Fig. 6, the interval between two waypoints is increased from 0.6 m to 1.0 m. As we can see in the figure, when transmitters are randomly placed in a square with 5 m edge length, the localization error is still smaller than 1 m with 90%, but for 10 m the localization error is reduced from 5 m to around 2.5 m. For 15 m and 20 m, around 90% of the localization errors are smaller than 5 m and 10 m, respectively, which are much smaller than that in Fig. 5. By increasing the moving area, we can efficiently reduce the localization error.

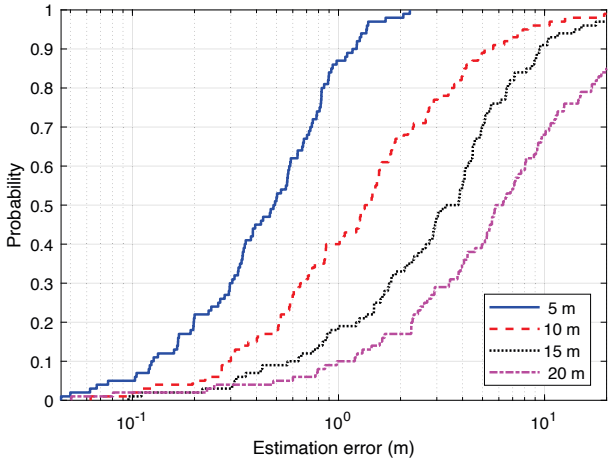

Fig. 5. CDF of localization error with robot trajectory $l_x = l_u = 0.6$ m.

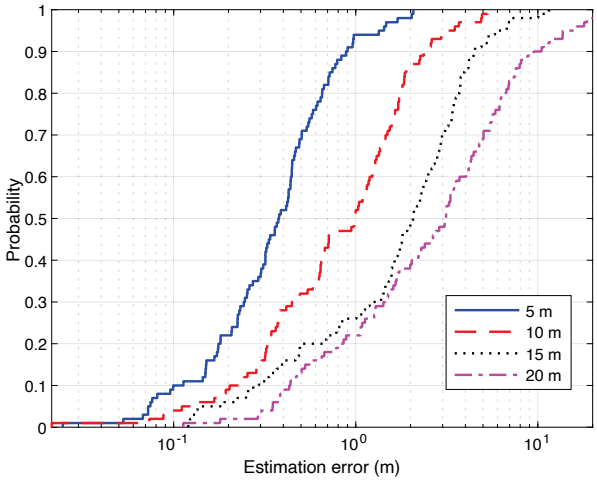

Fig. 6. CDF of localization error with robot trajectory $l_x = l_y = 1.0$ m.

To evaluate the performance of existing solutions, we implement the static localization algorithm (SLA) without knowing the path loss exponent in [13]. The SLA algorithm does not consider spatial correlation and relies on widely separated anchors. This algorithm is not suitable to directly solve the problem in this paper. However, to the best of our knowledge, there is no similar work that has been done and [13] is a classical work. We consider two scenarios: 1) the anchors are placed at the same location as the robot waypoints (sensor array 1 in Fig. 8, and 2) the anchors are placed at (20, 20), (20, 0), (0, 20), (0, 0), and (10, 10) (sensor array 2 in Fig. 8). For the first scenario, the location of anchors is the same as

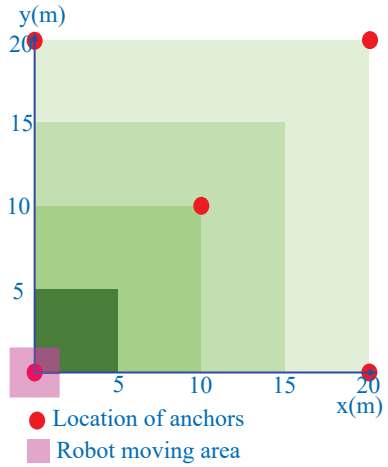

Fig. 7. Illustration of the robot moving area and the random source location. The sources are randomly generated based on the range. Four different areas are considered with edge lengths 5 m, 10 m, 15 m, and 20 m. The bigger squares overlap with the smaller squares. The five red dots are the locations of the anchor nodes which are used to evaluate the SLA.

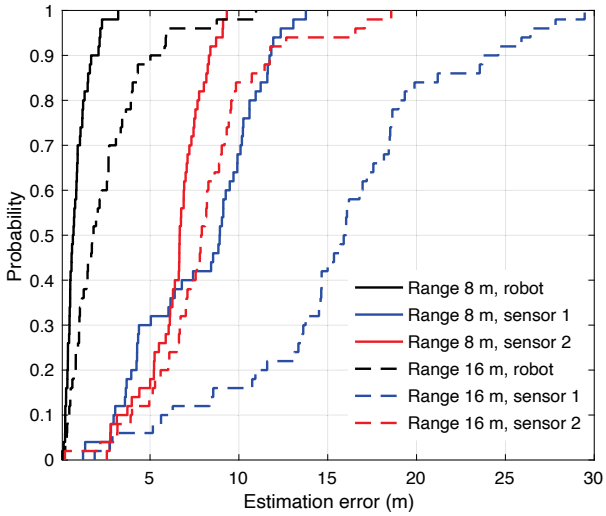

Fig. 8. CDF of location error: $l_x = l_y = 1.0$ m. The sensor array 1 and sensor array 2 are static sensor arrays using SLA. For sensor array 1: the anchors are placed at the same location as the robot waypoints; for sensor array 2: the anchors are placed at (20, 20), (20, 0), (0, 20), (0, 0), and (10, 10).

the robot moving area in Fig. 7. For the second scenario, the location of anchors is displayed using red circles in Fig. 7. As we can see from Fig. 8, the performance uses a static sensor array at the same location as the robot waypoints (sensor 1) is worse than that using a mobile robot with the proposed approach in this paper. When the transmitters are randomly distributed in a square with an edge of 8 m, 90% of the estimation error using a robot is smaller than 2 m, while for the sensor array 1 case it is around 8 m. For the edge length of 16 m, we have similar observations and performance of sensor array 1 becomes even worse. For the sensor array 2 case, the performance of 8 m and 16 m edges are similar since the anchor sensors are widely distributed. This

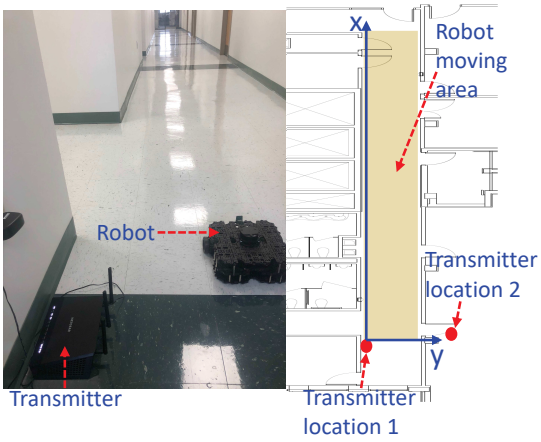

Fig. 9. Robot RSS data collection setup. The transmitter location 2 is behind a door and measurements are collected when the door is closed.

paper considers a more complex channel model with spatial correlations, whereas the SLA considers a log-normal channel model, where the solution relies on a bisection search. It is expected that better performance of SLA can be obtained if more computation resources are used.

We use a mobile robot to collect Wi-Fi RSS data and localize a transmitter (Wi-Fi router). TurtleBot3 Waffle Pi with Raspberry Pi 3B is used to receive Wi-Fi signals from an AC1750 NETGEAR Wi-Fi router. Secure Shell (SSH) is used to connect over the shared Wi-Fi network with the Raspberry Pi 3B that sits remotely on the Turtlebot3 Waffle Pi, which is over the floor of the experiment area. Once access to the Unix terminal in the Raspberry Pi 3B is granted through SSH, the directories containing the shell script can be accessed. The script is run to collect data over various points, after which the saved files are retrieved and collated. We process the collected RSS data offline in MATLAB.

An illustration of the data collection is shown in Fig. 9. The left-hand side shows the robot and the router, and the right-hand side shows the robot moving area along a corridor. The transmitter is placed at Location 1 in the corridor. The robot waypoints are shown in Fig. 10. The robot receives around 2.7 RSS measurements per second. The robot stays at each waypoint for 10 seconds and only the first 20 measurements are used. There are 5×4 waypoints with $l_x = l_y = 0.305$ m for the robot waypoints 1, 2, and 3, and with $l_x = 1.220$ m and $l_y = 0.305$ m for the robot waypoints 4 and 5. The angle θ_s is set as $2\pi/3$. As shown in Fig. 10, the estimated error is around 2 m, which is consistent with the numerical simulation. Also, we placed the transmitter at Location 2 in Fig. 9. The localization error is similar as shown in Fig. 11.

The developed algorithm finds a large number of robotic applications. First, the transmitter can be regarded as a reference robot that does not move and periodically sends out beacons. A swarm of task robots can use the estimated relative location with respect to the reference robot to navigate in a complex environment, such as pipeline inspection robots [27]. Second,

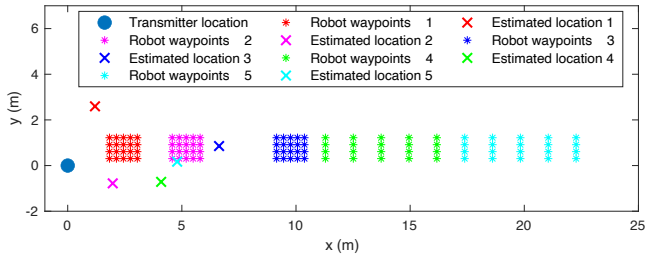

Fig. 10. Estimated location and robot waypoints. The transmitter is placed at the transmitter Location 1 in Fig. 9.

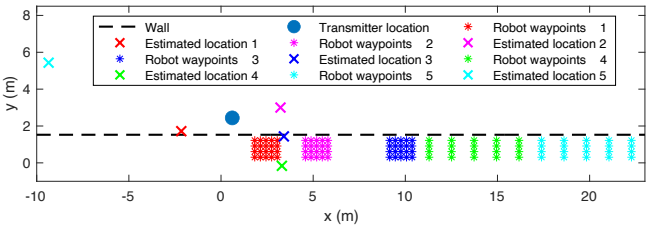

Fig. 11. Estimated location and robot waypoints. The transmitter is placed at the transmitter Location 2 in Fig. 9.

it can also be used for target searching with knowledge of the transmission power (or the received power at 1 m away from the transmitter) in complex unknown environments.

V. Conclusion

It is challenging for a robot using off-the-shelf single-antenna radios to localize a target. This paper develops a localization framework for a mobile robot using Received Signal Strength (RSS) in complex unknown environments. The robot moves along a predefined trajectory and collects RSS data at waypoints, which are used to estimate the wireless channel parameters, including spatial correlation, multipath fading, path loss exponent, and the distance from the transmitter. The channel model is then used to estimate the angle of arrival and the location of the transmitter. Numerical simulations and experiments are conducted to evaluate the performance of the proposed localization framework.

References

[1] M. Erdelj, E. Natalizio, K. R. Chowdhury, and I. F. Akyildiz, "Help from the sky: Leveraging uavs for disaster management," *IEEE Pervasive Computing*, vol. 16, no. 1, pp. 24–32, 2017.

[2] H. Guo and A. A. Ofori, "The internet of things in extreme environments using low-power long-range near field communication," *IEEE Internet of Things Magazine*, vol. 4, no. 1, pp. 34–38, 2021.

[3] M. Kotaru, K. Joshi, D. Bharadia, and S. Katti, "Spotfi: Decimeter level localization using wifi," in *Proceedings of the 2015 ACM Conference on Special Interest Group on Data Communication*, 2015, pp. 269–282.

[4] D. Vasisht, S. Kumar, and D. Katabi, "Decimeter-level localization with a single wifi access point," in *13th {USENIX} Symposium on Networked Systems Design and Implementation ({NSDI} 16)*, 2016, pp. 165–178.

[5] R. Ayyalasomayajula, A. Arun, C. Wu, S. Sharma, A. R. Sethi, D. Vasisht, and D. Bharadia, "Deep learning based wireless localization for indoor navigation," in *Proceedings of the 26th Annual International Conference on Mobile Computing and Networking*, 2020, pp. 1–14.

[6] X. Guo, L. Li, F. Xu, and N. Ansari, "Expectation maximization indoor localization utilizing supporting set for internet of things," *IEEE Internet of Things Journal*, vol. 6, no. 2, pp. 2573–2582, 2018.

[7] X. Wang, L. Gao, and S. Mao, "Biloc: Bi-modal deep learning for indoor localization with commodity 5ghz wifi," *IEEE access*, vol. 5, pp. 4209–4220, 2017.

[8] Y. Shu, C. Bo, G. Shen, C. Zhao, L. Li, and F. Zhao, "Magicol: Indoor localization using pervasive magnetic field and opportunistic wifi sensing," *IEEE Journal on Selected Areas in Communications*, vol. 33, no. 7, pp. 1443–1457, 2015.

[9] Y. Sun, M. Liu, and M. Q.-H. Meng, "Wifi signal strength-based robot indoor localization," in *2014 IEEE International Conference on Information and Automation (ICIA)*. IEEE, 2014, pp. 250–256.

[10] Y. Zou and H. Liu, "Rss-based target localization with unknown model parameters and sensor position errors," *IEEE Transactions on Vehicular Technology*, 2021.

[11] H. Lohrasbipeydeh and T. A. Gulliver, "Unknown rssd-based localization crlb analysis with semidefinite programming," *IEEE Transactions on Communications*, vol. 67, no. 5, pp. 3791–3805, 2019.

[12] R. Sari and H. Zayyani, "Rss localization using unknown statistical path loss exponent model," *IEEE Communications Letters*, vol. 22, no. 9, pp. 1830–1833, 2018.

[13] M. R. Gholami, R. M. Vaghefi, and E. G. Ström, "Rss-based sensor localization in the presence of unknown channel parameters," *IEEE Transactions on Signal Processing*, vol. 61, no. 15, pp. 3752–3759, 2013.

[14] C. Liang and F. Wen, "Received signal strength-based robust cooperative localization with dynamic path loss model," *IEEE Sensors Journal*, vol. 16, no. 5, pp. 1265–1270, 2015.

[15] L. Zhang, B. Yang, and X. You, "Received signal strength indicator-based recursive set-membership localization with unknown transmit power and path loss exponent," *IEEE Sensors Journal*, 2021.

[16] F. Bernardini, A. Buffi, D. Fontanelli, D. Macii, V. Magnago, M. Marracci, A. Motroni, P. Nepa, and B. Tellini, "Robot-based indoor positioning of uhf-rfid tags: The sar method with multiple trajectories," *IEEE Transactions on Instrumentation and Measurement*, vol. 70, pp. 1–15, 2020.

[17] A. Motroni, P. Nepa, P. Tripicchio, and M. Unetti, "A multi-antenna sar-based method for uhf rfid tag localization via ugv," in *2018 IEEE International Conference on RFID Technology & Application (RFID-TA)*. IEEE, 2018, pp. 1–6.

[18] A. Motroni, P. Nepa, V. Magnago, A. Buffi, B. Tellini, D. Fontanelli, and D. Macii, "Sar-based indoor localization of uhf-rfid tags via mobile robot," in *2018 International Conference on Indoor Positioning and Indoor Navigation (IPIN)*. IEEE, 2018, pp. 1–8.

[19] C. R. Karanam, B. Korany, and Y. Mostofi, "Magnitude-based angle-of-arrival estimation, localization, and target tracking," in *2018 17th ACM/IEEE International Conference on Information Processing in Sensor Networks (IPSN)*. IEEE, 2018, pp. 254–265.

[20] M. Malmirchegini and Y. Mostofi, "On the spatial predictability of communication channels," *IEEE Transactions on Wireless Communications*, vol. 11, no. 3, pp. 964–978, 2012.

[21] M. Gudmundson, "Correlation model for shadow fading in mobile radio systems," *Electronics letters*, vol. 27, no. 23, pp. 2145–2146, 1991.

[22] R. M. Vaghefi and R. M. Buehrer, "Received signal strength-based sensor localization in spatially correlated shadowing," in *2013 IEEE International Conference on Acoustics, Speech and Signal Processing*. IEEE, 2013, pp. 4076–4080.

[23] Z.-Q. Luo, W.-K. Ma, A. M.-C. So, Y. Ye, and S. Zhang, "Semidefinite relaxation of quadratic optimization problems," *IEEE Signal Processing Magazine*, vol. 27, no. 3, pp. 20–34, 2010.

[24] J. Turkka and M. Renfors, "Path loss measurements for a non-line-of-sight mobile-to-mobile environment," in *2008 8th International Conference on ITS Telecommunications*. IEEE, 2008, pp. 274–278.

[25] H. J. Jo and S. Kim, "Indoor smartphone localization based on los and nlos identification," *Sensors*, vol. 18, no. 11, p. 3987, 2018.

[26] Z. Xiao, H. Wen, A. Markham, N. Trigoni, P. Blunsom, and J. Frolik, "Non-line-of-sight identification and mitigation using received signal strength," *IEEE Transactions on Wireless Communications*, vol. 14, no. 3, pp. 1689–1702, 2014.

[27] H. Guo and A. A. Ofori, "Sequential task allocation with connectivity constraints in wireless robotic networks," in *2021 17th International Conference on Distributed Computing in Sensor Systems (DCOSS)*. IEEE, 2021, pp. 420–428.